J. Membrane Biol. 13, 353–386 (1973)

The Effect of Potassium Diffusion through the Schwann Cell Layer on Potassium Conductance of the Squid Axon

Gerold Adam

Fachbereich Biologie, Universität Konstanz, Germany

Received 10 April 1973

Summary. The accumulation of K^+ ions in the intermembranous spaces of the Schwann cell layer during K^+ ion current flow may lead to appreciable changes of the K^+ equilibrium potential. Thus, for an evaluation of the K^+ conductance of the axolemma, the transport of K^+ ions through the Schwann cell layer has to be characterized quantitatively. In the present work this is done for a simplified model of the geometrical arrangement of the slit-like channels traversing the Schwann cell region.

The K^+ transport through the slits is treated for two cases: (a) Assuming that electro-kinetic volume flow does not affect K^+ transport. In this case, pure diffusion of K^+ ions accounts for their removal from the intermembranous spaces. Estimates on electro-kinetic volume flow show that this case applies to axons of *Loligo forbesi* in voltage clamps of fairly small depolarizations. (b) For the case of appreciable electro-kinetic volume flow, evidence is adduced that its main effect is a widening of the slits through the Schwann cell layer. This physical situation could be treated only for the steady-state of convective diffusion of K^+ ions in the slits.

This case is applied to experiments on large depolarizing voltage clamps for *Loligo pealii axons*. It is shown that a widening of the slits to up to eight times the resting width is to be expected.

In both cases (a) and (b), marked deviations of the K^+ conductance of the axolemma from the Hodgkin-Huxley conductance result. The series resistance of the Schwann cell layer and the decay of after-effects of trains of action potentials are described by the theory.

Many attempts at a quantitative mechanistic description of axonal excitation processes have been devoted to the delayed or potassium conductance of the squid axon (Adam, 1970, 1971; Blumenthal, Changeux & Lefevre, 1970; Hill & Chen, 1970, 1971). However, the following serious difficulty arises in any comparison of a mechanistic theory of the K^+ conductance of the axolemma with the experimental K^+ current. Following the procedure of Hodgkin and Huxley (1952*d*), usually an experimental K^+ conductance is derived from the experiments by using the K^+ equilibrium potential of the resting axon. This phenomenological K^+ conductance is a conductance per-

taining to the entire aggregate of axolemma plus surrounding Schwann cell layer (SCL). It does not necessarily represent the K^+ conductance of the axolemma proper. In fact, appreciable effects of potassium diffusion polarization in the SCL are observed. For instance, Frankenhaeuser and Hodgkin (1956) have studied the after-effects of trains of action potentials and were able to ascribe those to an accumulation of K^+ ions in the region just outside the axolemma. For a quantitative description of these effects Frankenhaeuser and Hodgkin (1956) have postulated the existence of a water-filled space of about 300 Å thickness adjacent to the axolemma with a barrier of a permeability of about 6×10^{-5} cm/sec between this space and the extra-axonal medium. This empirical conception is known as the "Frankenhaeuser-Hodgkin space" and has proven to be very useful for understanding the effects of K^+ diffusion polarization, observed for small net currents. As Frankenhaeuser and Hodgkin (1956) pointed out already, this phenomenological device is not to be taken as an anatomical space. In fact, the structural correlate to the Frankenhaeuser-Hodgkin space is the entire SCL with its system of intermembranous spaces. These studies have been restricted to fairly small net K^+ currents.

Experimental results for larger K^+ currents are reported by Adelman and Palti (1972). They show that in a typical depolarizing voltage clamp experiment with a current of a few mamp per cm^2 and about 20-msec duration even larger effects can be observed, amounting to a shift in the K^+ equilibrium potential by as much as 40 to 50 mV, as can be derived from the tail currents after repolarization. To describe such effects, Adelman and Palti (1969, 1972) have used essentially the same empirical model of the SCL as Frankenhaeuser and Hodgkin (1956). This model is of course a very crude approximation of the geometrical structure of intermembranous spaces of the SCL. Furthermore, both these treatments did not consider the possible consequences of the electro-kinetic effects on the accumulation of K^+ ions in the SCL. As is shown later, because of the small intermembranous spaces of the SCL, the volume flow due to electric flow through the axolemma can give rise to appreciable effects. Thus, it is felt that the detailed regime of K^+ transport through the channels of the SCL has to be characterized quantitatively in order to evaluate the dependence on time and membrane potential of the K^+ concentration right outside the axolemma during a depolarizing voltage clamp.

As can be seen from the above results, the observed shift in the K^+ equilibrium potential is bound to give rise to substantial deviations of the K^+ conductance of the axolemma proper from the Hodgkin-Huxley (1952*d*) K^+ conductance. The aim of the present paper, therefore, is to describe

quantitatively on the basis of a detailed model of the SCL for voltage clamp experiments the changes of K^+ concentration right outside the axolemma and thus the changes of the K^+ equilibrium potential across the axolemma. With its use then the K^+ conductance of the axolemma proper is evaluated. This quantity, with respect to voltage and time dependence, turns out to be very much different from the Hodgkin-Huxley (1952*d*) conductance. It is shown, furthermore, that the voltage dependence of the steady-state axolemmal K^+ conductance is very similar for an axon in seawater to that in potassium-seawater, which seems to resolve the discrepancy between the Hodgkin-Huxley K^+ conductance and that for the axon in KCL-seawater as exhibited, for instance, by the representation of the steady-state voltage dependence, e.g. in Fig. 8 of Lecar, Ehrenstein, Binstock and Taylor (1967).

Physical Model of K^+ Transport through the SCL

Axon-Schwann Cell Structure

The structural relationship between axon and SCL of squid giant axon was first elucidated electron-microscopically by Geren and Schmitt (1954). They observed that the axolemma of *Loligo pealii* is surrounded by a layer of Schwann cells about 0.5 μm thick. In their micrographs, the Schwann cell membrane was observed to be separated from the axolemma by an intermembranous space of about 100 Å thickness. Following Cohen (1970), we shall in the following designate this structural intermembranous space as "Geren-Schmitt space" (GS space) and distinguish it from the empirical "Frankenhaeuser-Hodgkin space" mentioned above. As Geren and Schmitt (1954) already discovered, and Villegas and Villegas (1960*a*, *b*, 1968) elaborated in detail, the GS space is connected by slits of about 100 Å width with the outer surface of the Schwann cells. These slits follow a tortuous course through the SCL and represent extracellular spaces between two neighboring Schwann cells or between two processes of the same cell.

Villegas and Barnola (1961) and Villegas, Caputo and Villegas (1962) have worked out for the tropical squid *Doryteuthis plei* that the slit-like channels through the SCL represent the route of access of water-soluble substances such as glycerol from the extra-axonal space to the axolemma. Moreover, the penetration of colloidal thorium particles through these channels into the GS space has been demonstrated (Villegas & Villegas, 1964).

For *Doriteuthis plei*, the thickness of the GS space was determined as 80 Å, the width of the slits as 60 Å, their contour length as about 4.3 μm, and the fraction of axon surface these slits occupy as about 0.004 (Villegas *et al.*, 1962). Similar figures for the thickness of the GS space and for the width of the channels as given above for *Doriteuthis plei* can be evaluated for the Atlantic squid *Loligo* (Geren & Schmitt, 1954), the tropical squid

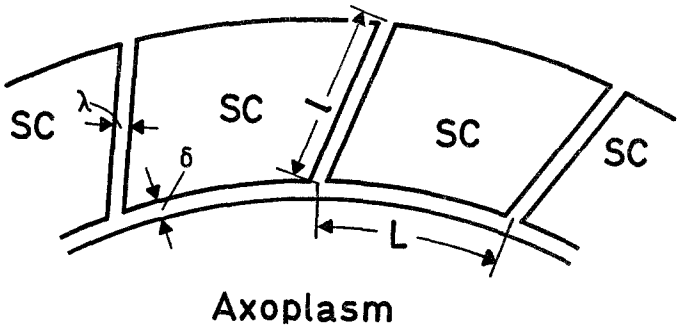

Fig. 1. Schematic representation of the Schwann cell layer. *SC* Schwann cell, *l* average length of the slits, λ width of the slits, *L* average distance of the slits, δ width of the Geren-Schmitt space between axolemma and Schwann cell layer

Sepioteuthis sepiodea (Villegas, 1968), and the Pacific squid *Dosidicus gigas* (Villegas & Villegas, 1968). However, the thickness of the SCL, and thus probably also the average length and fractional area of the slit-like channels is different for different species of squid (Caldwell & Keynes, 1960; Villegas & Villegas, 1968). Unfortunately, these latter geometrical characteristics have not been determined quantitatively for the Atlantic or Pacific species of squid.

Thus, the pertinent structure for understanding potassium accumulation near the axolemma is the GS space of about 80 Å between axolemma and surrounding Schwann cells. The GS space is connected by slit-like channels, 60 Å wide and presumably filled with a watery medium, with the space external to the SCL.

To proceed further, we consider a simplified structural model of the system of channels through the SCL. We replace the distribution of channels of different length by a system of unbranched channels all of equal length *l*, corresponding to the average length of the real channels (*see* Fig. 1). These channels may of course follow tortuous courses through the SCL and still allow the transport regime within them to be one-dimensional. The openings of these channels to the GS space are assumed to form a square net and thus be spaced at an average distance *L* so that the fraction *A* of axonal area the slits occupy is given by

$$A=\frac{2\lambda}{L}. \tag{1}$$

Here, λ is the width of the slits (*see* Fig. 1).

Estimates of the Contributions from Different Transport Mechanisms

The complete analysis of ion flow through a composite aggregate like the squid giant axon is considerably involved. However, certain realistic approximations can be introduced, simplifying the problem appreciably.

First of all, the membrane resistance of the Schwann cells is of the order of 1000 $\Omega\,cm^2$ and independent of the current flow; from these and other results it can be concluded "that the channels crossing the glia cells are the main pathways for rapid diffusion of ions between the external solution and the axonal and neuronal surfaces" (Villegas, 1972).

For a full analysis of ion flow through the slit-like channels one would have to evaluate the profile along the slits of the electric field and of the transference numbers of the ionic species present, in particular of potassium. Of course, these quantities vary with the ionic concentrations, and thus depend on time and voltage, for instance because of accumulation of potassium in the intermembranous spaces. Thus, the full treatment of ionic flow in the slits, including the dependence of the diffusion potentials on time and length coordinate, represents a very involved problem. However, in a good approximation it can be avoided for the following reasons. In all cases of interest here, there is a considerable excess of other ions in addition to K^+ ions, precluding the build-up of an appreciable potential gradient along the channels. As Frankenhaeuser and Hodgkin (1956) noted in this context, the junction potential between 500 mM KCl and 500 mM NaCl is only about 5 mV. Thus, the electric potential drop along the slits is essentially that across the series resistance due to the SCL.

Furthermore, very little of the electric current through the slits will be carried by K^+ ions. In the resting state, for instance, the concentration ratio of sodium to potassium is about fifty. During K^+-accumulation, this ratio decreases. However, even a ratio of about one would introduce an error of only about 15% in the K^+ diffusion flow, as can be inferred from calculations on electrode kinetics (Vetter, 1961) or estimated from the concentrations and mobilities of all the anions and cations present. Within the accuracy possible in the present paper, we thus may neglect the migration of K^+ ions due to an electric potential gradient along the slits as compared to diffusion along the concentration gradient.

As discussed by Barry and Hope (1969), electro-kinetic effects might play an important role in ion transport near cell membranes. In the following their contribution is estimated. Vargas (1968) has shown for *Dosidicus gigas* giant axons that there is an appreciable volume flow, connected with the electric current. The flow of (electroneutral) solute, on the other hand, is comparably small (Vargas, 1968). The volume flow connected with current flow is essentially flow of water. The relevance of this electro-kinetic effect can be estimated as follows. Neglecting the contribution of any solute flow not associated with the electric current, as seems justified from the experimental results of Vargas (1968) for giant axons of *Dosidicus gigas*, and as is

valid also for plant cells (Barry & Hope, 1969), the phenomenological equations read (*cf.* Schlögl, 1964):

$$I = L_E E + L_{EP} P, \tag{2}$$

$$q = L_{EP} E + L_P P. \tag{3}$$

Here, I is the electric current, L_E the membrane conductance, E the change of membrane potential from the resting state, P the pressure difference across the axolemma, L_{EP} the electro-osmotic coefficient, q the volume flow through the axolemma, and L_P the filtration coefficient.

Vargas (1968) measured the streaming potential upon applying a hydrostatic pressure to the inside of *Dosidicus* giant axons. In 22 experiments with seawater or KCl-seawater as the external medium he obtained as an average

$$L_{EP}/L_E = (4.1 \pm 0.5) \times 10^{-5} \text{ Volt per cm } H_2O \text{ of pressure.} \tag{4}$$

With $L_E \sim 0.001\ \Omega^{-1}\ \text{cm}^{-2}$ for the axon in seawater at the resting potential:

$$L_{EP,\,\text{seaw.}} \sim 4.2 \times 10^{-4}\ \text{cm}^3/\text{cm}^2\ \text{sec V}. \tag{5}$$

Here and in the following, the units cm^3/cm^2 sec (instead of cm/sec) were chosen to indicate clearly the physical meaning, i.e. volume flux in cm^3 per cm^2 axon surface and second.

With $L_E \sim 0.008\ \Omega^{-1}\ \text{cm}^{-2}$ for the axon in KCL-seawater, i.e. for a depolarized axon (Rojas & Ehrenstein, 1965):

$$L_{EP,\,\text{KCl-seaw.}} \sim 3.3 \times 10^{-3}\ \text{cm}^3/\text{cm}^2\ \text{sec V}. \tag{6}$$

Unfortunately, these numbers pertain to a species of squid different from those discussed later in this paper. However, to get an idea of the order of magnitude of this electro-kinetic effect for *Loligo* axons, we shall base the following estimates on these figures.

In a voltage clamp experiment $P = 0$. Accordingly the volume flux within the time t is

$$q \cdot t = L_{EP} \cdot E \cdot t. \tag{7}$$

In our later application of the transport model to voltage clamp experiments on *Loligo forbesi* giant axons, the depolarizations from the resting state are quite small, $E \cdot t$ amounting to maximally 8×10^{-4} V sec. With the numbers given above, one obtains $q \cdot t \sim 3.4 \times 10^{-7}$ to $2.6 \times 10^{-6}\ \text{cm}^3$ per cm^2 axon surface. Compared with the volume $A \cdot l$ of the slits of $10^{-5}\ \text{cm}^3$

per cm^2 axon surface, as determined in a later section for *Loligo forbesi* axons, the volume flux amounts only to maximally 1/30 to 1/4 of the slit volume.

In contrast, our later applications to axons from the species *Loligo pealii*, with depolarizations of up to 120 mV and about 20 msec duration, may result in $q \cdot t \sim 10^{-6}$ to 8×10^{-6} cm^3 per cm^2 axon surface. This is quite comparable to the slit volume of about $A \cdot l \sim 5 \times 10^{-6}$ cm^3 per cm^2 axon surface, as determined later.

The electro-osmotic volume flow might lead to at least two distinct effects. It might give rise to a convection flow of ions in the slits superimposed on the diffusion flow. In addition, it might give rise to a change of the geometrical dimensions of the intermembranous spaces in the SCL, for instance, to a widening of the slits. The following estimates point to the latter effect as the main consequence of volume flow.

If the boundary membranes of the slits were rigid walls, only the first mentioned effect could take place. In this case the volume flow through the axolemma gives rise to viscous flow of a watery electrolyte medium through the narrow slits. For this hypothetical case, we are able to calculate the pressure difference Δp between both ends of a slit, which is necessary to maintain the observed volume flow. Applying the treatment of viscous flow between rigid parallel plates (*cf.* Gerthsen, 1963), we obtain for the average velocity $\bar{u}$ of viscous flow in the slits of length l and width λ:

$$\bar{u} = \frac{\Delta p \cdot \lambda^2}{12\eta \cdot l}. \tag{8}$$

Here, η is the viscosity of the electrolyte solution in the slits. Since the volume flow is

$$q = \bar{u} \cdot A$$

one obtains

$$\Delta p = \frac{12q \cdot \eta \cdot l}{A \cdot \lambda^2}. \tag{9}$$

Using $\eta = 0.015$ poise, $l = 5 \times 10^{-4}$ cm, $A = 0.01$, $\lambda = 6 \times 10^{-7}$ cm, and $q \sim 5 \times 10^{-5}$ to 4×10^{-4} cm^3/cm^2 sec, as used above for *Loligo pealii*:

$$\Delta p \sim 1.25 \times 10^6 \text{ to } 1 \times 10^7 \text{ dyne/cm}^2. \tag{10}$$

Thus, enormous pressure differences are the result in this hypothetical case. It is extremely unlikely that upon pressure differences of up to ten atmospheres the membranes of the slits behave like rigid walls. On the

contrary, it appears safe to assume that the membranes enclosing the intercellular spaces bulge according to the volume flow through the axolemma. Thus, the main effect of volume flow is expected to be a change of the geometrical parameters of the intermembranous spaces. Since the area of the walls of the slits is much larger than the cross-section of the slits of the membrane area bordering the GS space, the main effect of an isotropic pressure built up in the system of intermembranous spaces would be a widening of the slits crossing the SCL.

We may sum up the results of the above estimates on the effect of electrokinetic volume flow as follows. In the absence of experimental data on the electro-osmotic coefficient L_{EP} for *Loligo* axons, unfortunately only rough estimates based on data for *Dosidicus* axons, can be made. For depolarizations $\leqq 45$ mV, as applies to electrophysiological data used later for *Loligo forbesi*, the effect of electro-kinetic volume flow seems to be very small and will be neglected in the following. Thus, pure diffusion in a system of rigid slits is assumed to be the transport regime in these cases. For the larger depolarizations in the case of *Loligo pealii* axons, the electroosmotic volume flow is appreciable and will be accounted for later by allowing the geometry of the slits to be a function of volume flux through the axon membrane.

Treatment of Diffusion without Convection in the Slits of the SCL

As was discussed above, under certain circumstances the effect of volume flow through the slits of the SCL may be neglected. For an axon in seawater containing tetrodotoxin, the course of events during a depolarizing voltage clamp then is the following. Upon depolarization of the axolemma, the K^+ conductance turns on, K^+ ions traverse the axolemma and redistribute in the GS space. Thereby the K^+ concentration in this space rises and creates a concentration gradient along the slits. The transport of K^+ ions by diffusion through the slits is now to be formulated quantitatively.

Comparison of Diffusion Times in the GS Space and in the Channels

A natural approximation for the arrangement of equidistant openings of the slit-like channels to the GS space is a square net. The relaxation time τ_{GS} for concentration redistribution within a square parallelepiped of GS space of length L is about:

$$\tau_{GS} \approx L^2/2\pi^2 D \tag{11}$$

where D is the diffusion coefficient (Carslaw & Jaeger, 1959). Later in this paper it will be shown that the time constant τ_{Ch} of concentration redistribu-

tion in the channels is about

$$\tau_{Ch} \approx l^2/\alpha_1^2 D \tag{12}$$

where l is the length of a channel, and α_1 is the first root of the characteristic Eq. (25).

Thus, using Eq. (1):

$$\frac{\tau_{GS}}{\tau_{Ch}} = \frac{2\alpha_1^2 \lambda^2}{\pi^2 A^2 l^2}. \tag{13}$$

With the figures obtained by Villegas *et al.* (1962), i.e. $A = 0.0041$, $l = 0.00045$ cm, $\lambda = 6 \times 10^{-7}$ cm, yielding $\alpha_1 = 1.10$, one obtains $\tau_{GS}/\tau_{Ch} \approx 0.026$.

With the figures used later for *Loligo forbesi*, i.e. $A = 0.01$, $l = 0.001$ cm, $\lambda = 6 \times 10^{-7}$ cm, yielding $\alpha_1 = 1.455$, the ratio is $\tau_{GS}/\tau_{Ch} \approx 1.5 \times 10^{-3}$. Similar figures pertain to the parameters used later for *Loligo pealii*.

Thus, in all cases of interest in the present paper, the redistribution of K^+ ions in the GS space is very much faster than the redistribution of K^+ ions in the channels. Therefore, the K^+ concentration in the GS space may be considered approximately uniform at every instant during the diffusion process in the channels.

Basic Differential Equations

The one-dimensional diffusion through the channels in the SC layer is described by:

$$\frac{\partial c}{\partial t} = D \frac{\partial^2 c}{\partial x^2} \tag{14}$$

where t is the time, D the diffusion coefficient, x the length coordinate along the channel, being zero at the outer border of the SCL and $x = l$ at the openings to the GS space. Further,

$$c = K_e - K_{eo} \tag{15}$$

is the excess of the K^+ concentration K_e over the resting value K_{eo}.

In this formulation K_{eo} may be a time-independent linear function of x, allowing for a small resting efflux of K^+ ions through the channels, which may be carried partly by the resting efflux of K^+ from the axoplasm and partly by shifts of K^+ ions due to activities of the Schwann cells. In such a case $c\,(x, t)$ describes the excess of K^+ concentration above the liuear resting concentration gradient for K^+ ions in the channels.

The initial condition is in the case of a depolarizing voltage clamp:

$$t=0\colon c=0. \tag{16}$$

The boundary conditions are:

$$x=0\colon c=0 \tag{17}$$

$$x=l\colon \delta\frac{\partial c}{\partial t}=\frac{I_K(t)}{F}-AD\frac{\partial c}{\partial x} \tag{18}$$

where δ is the thickness of the GS space, $I_K(t)$ the time-dependent K^+ current, F the Faraday constant, and A the fraction of axon surface occupied by the openings of the slit-like channels.

The time-dependent boundary condition (18) describes the balance of K^+ ions in the GS space and introduces the only analytical involvement of the otherwise straightforward one-dimensional diffusion problem. In a depolarizing voltage clamp experiment, the time-dependent K^+ current $I_K(t)$ may be described phenomenologically by the Hodgkin-Huxley formation (1952*d*):

$$I_K(t)=I_\infty(1-\rho e^{-t/\tau})^4. \tag{19}$$

In this context, Eq. (19) is nothing but an empirical expression of the electrical current carried by K^+ ions through the axon membranes, as measured in a depolarizing voltage clamp in the presence of tetrodotoxin, for instance.

Similarly, in the case of repolarization after a depolarizing voltage clamp, the time-dependent K^+ current in Eq. (18) may be described (Hodgkin & Huxley, 1952*d*) by:

$$I_K(t)=I_\infty e^{-t/\tau}. \tag{20}$$

In this case, the initial condition is different from Eq. (16).

Allowance for a small but nonzero repolarization current at $t=\infty$ is not necessary here, because it does not affect the major part of the time course of the repolarization current, which is sufficient for the present purposes.

Solutions of the Diffusion Equation for Depolarization

In Appendix I, the solution of Eqs. (14) through (19) for immediate onset of the K^+ current, i.e. for $\tau=0$, is shown to be:

$$c_0(x,t)=d\cdot x-\sum_{n=1}^{\infty}2d\cdot l\frac{\sin(\alpha_n x/l)}{N(\alpha_n)\sin\alpha_n}e^{-K_n t} \tag{21}$$

where

$$N(\alpha_n)=\frac{\delta\cdot\alpha_n^2}{A\cdot l}\left(1+\frac{\delta\alpha_n^2}{A\cdot l}\right)+\alpha_n^2 \tag{22}$$

$$K_n=D\alpha_n^2/l^2 \tag{23}$$

$$d=I_\infty/FAD \tag{24}$$

and α_n are the roots of

$$\alpha\,\mathrm{tg}\,\alpha=\frac{lA}{\delta}. \tag{25}$$

In Fig. 2*A*, we have plotted c_o versus x/l for different times t, as given by the curve parameters. In Fig. 2, the following parameters were used. Assuming, that the channels are filled with watery electrolyte solution, we have at $T=20$ °C a diffusion coefficient of $D=1.7\times10^{-5}$ cm^2/sec. The geometrical parameters applied were: $A=0.01$, $l=0.001$ cm, $\delta=80$ Å. Fig. 2*A* shows the filling-up of the channels after a constant K^+ current is switched on instantaneously at $t=0$.

The reverse process of draining of K^+ ions from the channels after a sudden stop of the K^+ current is described by Eqs. (14), (16) and (17). In addition, the boundary condition Eq. (18) is to be used with $I_K(t)=0$; and the initial condition is

$$t=0\colon c=d\cdot x. \tag{26}$$

The corresponding solution is simply given [*see* Eq. (28)] by:

$$c=d\cdot x-c_0. \tag{27}$$

This result is plotted in Fig. 2*B* for the same parameters as used in Fig. 2*A*.

The solution for the complete set of Eqs. (14) through (19) is derived in Appendix I as:

$$c(x,t)=d\cdot x(1-\rho e^{-t/\tau})^4+\sum_{n=1}^{\infty}2\cdot l\cdot d\,\frac{\sin(\alpha_n x/l)}{\sin\alpha_n}\,\frac{e^{-K_n t}}{N(\alpha_n)}\left[\sum_{m=1}^{4}T_{mn}-dx(1-\rho)^4\right] \tag{28}$$

where

$$T_{mn}=(-\rho)^m\binom{4}{m}\frac{1-e^{-\left(\frac{m}{\tau}-K_n\right)t}}{\left(1-\frac{\tau}{m}K_n\right)}. \tag{29}$$

Again the α_n are the solutions of Eq. (25).

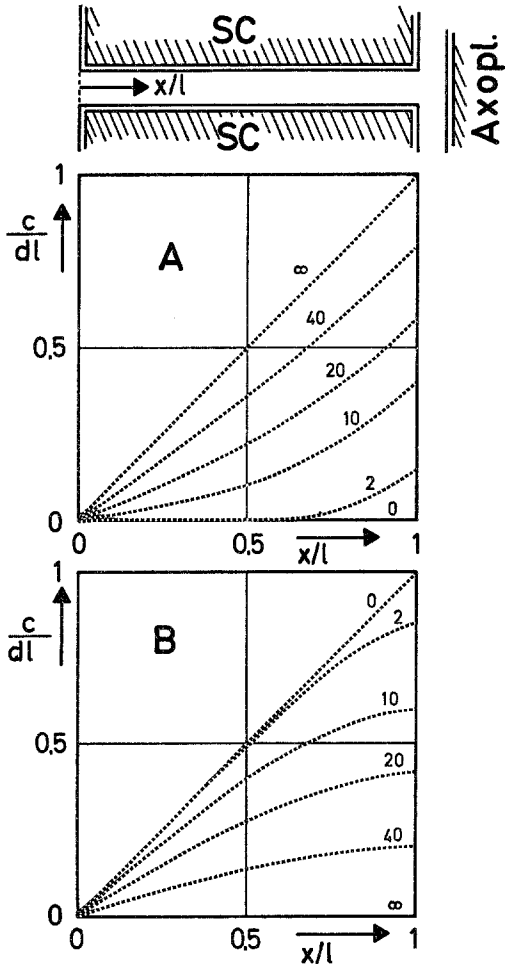

Fig. 2. Plot of the excess concentration of K^+ ions versus length coordinate of the slits (*see insert above*). (*A*) Time course of the concentration profile after an instantaneous step-up of K^+ current (according to Eq. (21) of the text). (*B*) Time course of the concentration profile following an instantaneous step-down of current after steady state of K^+ diffusion had been established (according to Eq. (27) of the text). Parameters used: $D=1.7 \times 10^{-5}$ cm^2/sec, $A=0.01$, $l=10$ μ, $\delta=80$ Å. Curve parameter: time in msec

Using the excess concentration $c(l, t)$ of K^+ ions in the GS-space, the axolemmal equilibrium potential for K^+ ions at every instant during the voltage clamp can be given by:

$$V_K(t)=\frac{RT}{F}\ln\left[\frac{K_{e_o}(l)+c(l,t)}{K_i}\right] \tag{30}$$

where $K_{e_o}(l)$ is the resting K^+ concentration in the GS space, K_i the axoplasmic K^+ concentration, and F the Faraday constant.

With the use of Eq. (30), the time-dependent K^+ conductance $g_K(t)$ of the axolemma proper can be evaluated as:

$$g_K(t)=I_K(t)/[V-V_K(t)] \tag{31}$$

where V is the membrane potential.

Application of the Theory to Experiments on Axons from *Loglio forbesi*

Depolarizing Voltage Clamp

The equations of the last section may be applied to phenomena of K^+ diffusion polarization in voltage clamp experiments of relatively small depolarizations. Frankenhaeuser and Hodgkin (1956) have reported such experiments for an axon at $T=8$ °C (*see* their Fig. 14*b* and Table 8). Actually, all experiments on K^+ diffusion polarization known to us for *Loligo forbesi* have used fairly small current densities. To describe these experiments we first discuss the theoretical parameters needed.

(a) The diffusion coefficient of KCl in aqueous solutions of an ionic strength comparable to seawater for $T=6$ to 8 °C is in the range $D=1.15\times 10^{-5}$ to 1.25×10^{-5} cm^2/sec (Landolt-Börnstein, 1969). We shall use these figures for K^+ diffusion in the slits of the SCL at $T=6$ and 8 °C. From the study of the ternary system H_2O/KCl/NaCl it is known that in the range of electrolyte concentrations of interest, the diffusion coefficient of KCl does not depend appreciably on the concentration ratio K^+/Na^+ (Landolt-Börnstein, 1969).

(b) The resting K^+ concentration $K_{e_o}(l)$ in the GS space is needed. One might want to use the figure for seawater. However, it was consistently observed for *Loligo forbesi* (Hodgkin & Huxley, 1952*b*) that the resting K^+ equilibrium potential is somewhat smaller than the theoretical one, which is computed from the axoplasmic and external medium concentrations of K^+ ions. As these authors pointed out, probably the resting K^+ concentration in the GS space is somewhat larger than that of seawater. This may be due to K^+ leakage from the axoplasm and possibly from the interior of the Schwann cells. Other explanations for the shift in "K^+ equilibrium-potential" of course are possible and have partly been discussed by the above authors, too.

To arrive at a consistent description, we allow for a small resting concentration gradient for K^+ ions along the slits. Then, the resting K^+ concentration $K_{e_o}(l)$ in the GS space can be evaluated from the resting K^+ equilibrium potential $V_{K_o}=-77$ mV as obtained electrophysiologically by Hodgkin and Huxley (1952*b*). Using $K_i=400$ mM and $T=8$ °C, one obtains from

$$K_{e_o}(l)=K_i\exp(FV_{K_o}/RT) \tag{32}$$

the figure

$$K_{eo}(l) = 16.66 \text{ mM}. \tag{33}$$

In a typical voltage clamp experiment, the accumulation of K^+ ions in the GS space is much larger than the difference between $K_{eo}(l) = 16.66$ mM and $K_{eo}(o) = 10$ mM (seawater). Thus, in most cases the use of the figure of Eq. (33) instead of the figure for seawater is not of much relevance. For small net currents, as for instance due to a train of action potentials (Frankenhaeuser & Hodgkin, 1956), this difference should be taken into account, however. For sake of consistency, we shall do this in all of the following examples.

(c) The resting potential of *Loligo forbesi* can be taken as $V_r = -65$ mV (Hodgkin & Huxley, 1952*a*).

(d) As to the geometrical characteristics of the SCL of giant axons from *Loligo forbesi*, only the width of the GS space $\delta = 80$ Å can be given with some confidence. The average length l of the channels and their fractional area A are not known from independent measurements. In the following these parameters will be fitted, so as to describe the experiments given by Frankenhaeuser and Hodgkin (1956) on their Fig. 14*b*.

In these experiments, the shifts of the K^+ equilibrium potential were determined during a voltage clamp of 36 mV depolarization at $T = 8$ °C. From the tail currents at 5.76 and 22 msec, shifts of V_{Ko} from the resting value of 9 and 24 mV, respectively, were derived (*see* Frankenhaeuser & Hodgkin, Table 8, l.c.). Thus, even from such a small depolarization with a concomitantly small clamp current of $I_\infty = 0.73$ mamp/cm^2, the conductance of the axolemma proper differs by 19% (for 5.76 msec) and by 50% (for 22 msec) from the phenomenological K^+ conductance evaluated in the usual way (Hodgkin & Huxley, 1952*d*). This result, based on direct experimental evidence, can be elaborated in more detail using the description of K^+ diffusion in the SCL as follows.

The time dependence of the depolarization current in their Fig. 14*b* and the net fluxes Q_K of K^+ ions given in Table 8 for the same axon (Frankenhaeuser & Hodgkin, 1956) can be well described by Eq. (19) with $I_\infty = 0.73$ mamp/cm^2, $\rho = 1$, and $\tau = 1.5$ msec.

In Table 1 the experimental shifts of the K^+ equilibrium potential (Table 8, l.c.) and the theoretical results computed from Eqs. (28) through (33) are given. Here the following parameters were used: $T = 8$ °C; $D = 1.25 \times 10^{-5}$ cm^2/sec; $V_r = -65$ mV; $V_{Ko} = -77$ mV, giving $K_{eo}(l) = 16.66$ mM; $\delta = 80$ Å; $V - V_r = 36$ mV; $I_\infty = 0.73$ mamp/cm^2; $\tau = 1.5$ msec; $\rho = 1$. The figures chosen for the parameters A and l are given in the Table.

Table 1. Parameters of K^+ diffusion polarization in giant axons of *Loligo forbesi* (depolarization of voltage clamp: 36 mV)

	$t=5.76$ msec			$t=22$ msec		
	V_K-V_{Ko} [mV]	$c(l)$ [mM]	g_K [mho/cm^2]	$V-V_{Ko}$ [mV]	$c(l)$ [mM]	g_K [mho/cm^2]
Experiment[a]	9	–	–	24	–	–
Theory[b]						
$A=0.01$; $l=10$ μm	9.9	8.4	0.0176	24.3	28.7	0.0308
$A=0.01$; $l=8$ μm	9.9	8.4	0.0176	24.1	28.4	0.0306
$A=0.01$; $l=5$ μm	9.9	8.4	0.0176	22.4	25.4	0.0286
$A=0.008$; $l=10$ μm	11.2	9.8	0.0182	27.3	34.7	0.0352
$A=0.012$; $l=8$ μm	8.9	7.4	0.0171	21.7	24.2	0.0278

[a] Taken from B. Frankenhaeuser and A. L. Hodgkin, *J. Physiol.* **131**:341 (1956), Table 8.
[b] Theory according to Eqs. (17) through (22) of the text, with $T=8$ °C; $D=1.25\times10^{-5}$ cm^2/sec; $\delta=80$ Å; $V_r=-65$ mV; $V_{Ko}=-77$ mV, giving $K_{eo}(l)=16.66$ mM; $V-V_r=36$ mV; $I_\infty=0.73$ mamp/cm^2; $\tau=1.5$ msec; $\rho=1$.

As can be seen, the choice $A\approx0.01$ and $l\approx0.001$ cm works well. Increasing A by about 10% and decreasing l by about 10% certainly would improve the fit. In view of the other uncertainties of the comparison with the experiments, this did not seem worth the effort, however.

As can be seen from Table 1, the K^+ equilibrium potential is much more sensitive to A than to l for the times t of interest here.

The figures $A\approx0.01$ and $l\approx10$ μm found above for *Loligo forbesi* are of the same order of magnitude as those determined by other methods for the tropical squid *Doryteuthis plei* (Villegas *et al.*, 1962).

Tentatively, we can expect values of about $A\approx0.01$ and $l\approx10$ μm as being characteristic for small voltage clamp currents on giant axons from *Loligo forbesi*. In this case, we are able to derive quantitatively the time dependence of the K^+ conductance of the axolemma proper from the observed K^+ current for small depolarizations. As a first example, we use the K^+ current as given by the Hodgkin-Huxley (1952*d*) equations for a voltage clamp with the moderate depolarization of $V-V_r=45$ mV. In this case the asymptotic current is $I_\infty=1.0$ mamp/cm^2, the parameter $\rho=0.620$, and the time constant in Eq. (19) $\tau=2.314$ msec. The Hodgkin-Huxley K^+ conductance for this depolarization as the curve labeled with 1 is plotted in Fig. 3. With a different ordinate scale, this is also the empirical course of the K^+ current with time, as described by Eq. (19). The theoretical time course of the axolemmal K^+ conductance according to Eqs. (28) through (33) is also

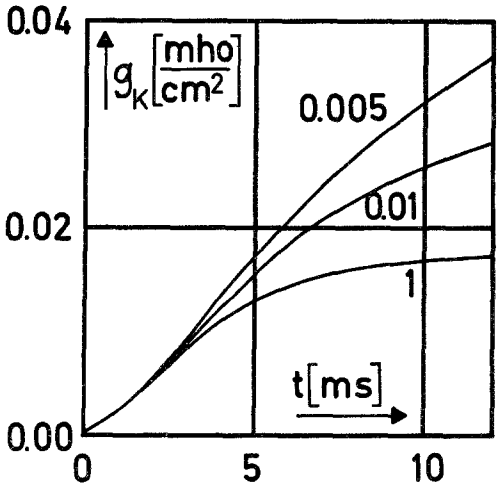

Fig. 3. Time course of the K^+ conductance of the axolemma during a depolarizing voltage clamp of $V-V_r=45$ mV, $I=1$ mamp/cm^2, $\rho=0.620$, $\tau=2.314$ msec. Here Eqs. (28) through (33) of the text were used. Parameters: $T=6$ °C; $D=1.15\times10^{-5}$ cm^2/sec; $V_{Ko}=-77$ mV; giving $K_{eo}(l)=16.28$ mM; $K_i=400$ mM; $\delta=80$ Å; $l>5$ μ. Curve parameter: A. Curve 1 is the Hodgkin-Huxley K^+ conductance, corresponding to $A=1$; $l\to0$

given in Fig. 3. Here, for a consistent description we observed that the Hodgkin-Huxley (1952*d*) parameters are reduced to $T=6$ °C, and therefore the following set of parameters is applicable: $T=6$°C; $V_{Ko}=-77$ mV, giving $K_{eo}(l)=16.28$ mM; $D=1.15\times10^{-5}$ cm^2/sec; $V_r=-65$ mV; $V-V_r=45$ V; $I_\infty=1.0$ mamp/cm^2; $\tau=2.314$ msec; $\rho=0.620$, $\delta=80$ Å. The para-parameters chosen A are given as curve parameters in Fig. 3. The parameter l must be larger than 5 μm such that its effect is negligible in the time range of Fig. 3.

In the absence of the SCL, i.e. in the case $A=1$ and $l\to0$, the theory yields the Hodgkin-Huxley conductance (*see* curve 1 in Fig. 3). As can be seen in Fig. 3, there are gross deviations of the K^+ conductance of the axolemma proper from the Hodgkin-Huxley conductance, if the parameters A and l are chosen in the range evaluated above for *Loligo forbesi*, and by Villegas *et al.* (1962) for *Dorytheutis plei.* Only in the induction period at small times is the effect of K^+ diffusion polarization negligible. Thus, any test of a molecular theory of the axolemmal K^+ conductance mechanism is bound to fail, if it is based on a comparison with the Hodgkin-Huxley K^+ conductance. For instance, Hill and Chen (1971) have put forward arguments against cooperative interactions in the structures of the axolemma that mediate the K^+ conductance. These arguments can not be conclusive be-

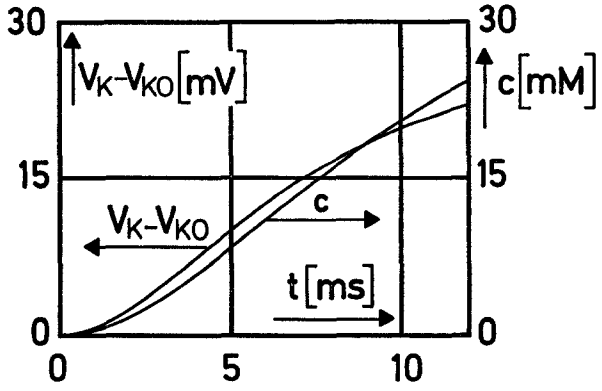

Fig. 4. Time course of the excess K^+ concentration c in the GS space and of the difference of the K^+ equilibrium potential V_K to the resting value V_{K_o}. Parameter $A=0.01$; other parameters are the same as in Fig. 3

cause the time course of the K^+ current is not given simply by that of the K^+ conductance, as these authors imply, but according to Eq. (31) it is determined by the time dependence of the K^+ conductance as well as by the time dependence of the K^+ equilibrium potential. Thus, the consequences of superposition of K^+ current curves, as observed by Cole and Moore (1960) have to be reevaluated by calculating the effect of K^+ accumulation in the GS space under the conditions of the superposition experiments.

Of course, the arguments of Hill and Chen (1971) concerning the behavior at short times, i.e. the "induction behavior", remain valid, because at short times the K^+ accumulation in the GS space is negligible. However, if one considers their curves allowing for a marked cooperativity, one notes very similar deviations from the noncooperative (Hodgkin-Huxley) curve, as are exhibited by our curves 0.01 or 0.005 on Fig. 3 compared to curve 1 (the Hodgkin-Huxley conductance). A quantitative evaluation of these aspects is under investigation now.

For further illustration of the physico-chemical characteristics of the GS layer, we have plotted in Fig. 4 the time courses of $[V_K(t)-V_{K_o}]$ and of $c(l, t)$, corresponding to curve 0.01 in Fig. 3. As can be seen, appreciable shifts in K^+ concentration in the GS space are to be expected even for a small depolarizing voltage clamp on *Loligo forbesi* giant axons.

In addition, Fig. 4 shows that the steady state of K^+ concentration in the GS space is not reached within the 12-msec duration of the voltage clamp. In fact, the redistribution times for K^+ ions in the channels are of the order of 30 msec, as will be shown in Fig. 6. The K^+ conductances shown in curves 0.01 and 0.005 in Fig. 3 have not

reached their steady states after 12 msec either. Of course, as long as the experimental K^+ current $I_K(t)$ can be described by Eq. (19), and this seems to be the case for *Loligo forbesi* and $t \leqq 11$ msec (Hodgkin & Huxley, 1952*d*), the axolemmal K^+ conductance can be evaluated straightforwardly by Eqs. (28) through (33). If one wants to know the K^+ conductance at longer times, the phenomenological description of $I_K(t)$ for $t > 12$ msec is needed. At these longer times of the voltage clamp, very often a decrease of K^+ current with time is observed. This effect can be seen in Fig, 14*b* of Frankenhaeuser and Hodgkin (1956), for instance. These authors have proposed already that this decrease is again an effect of K^+ accumulation in a region just outside the axolemma. This polarization effect is described by our theory of K^+ diffusion through the slits of the SCL, as follows. (A discussion in terms of the Frankenhaeuser-Hodgkin model was given by Adelman and Palti, 1972). Let us consider the case of Fig. 3, where the K^+ conductance of the axolemma rises much faster as corresponds to the K^+ redistribution time of the slits. Then at $t > 12$ msec the K^+ accumulation in the GS space proceeds, because the supply of K^+ ions from the axon interior is maintained by the nearly steady-state K^+ conductance. If this K^+ conductance of the axolemma changes only slowly with time, the continued increase of $c(l, t)$ and $V_K(t)$ according to Eqs. (30) and (31) must lead to a decrease of the current $I(t)$ with time. Quantitatively, this effect is to be described by Eqs. (14) through (19), where only Eq. (19) is to be supplemented by a term describing phenomenologically the decrease of $I_K(t)$ at long times. Unfortunately, in essentially all experimental studies this drop of $I_K(t)$ seems to have been considered only as a nuisance for the experimenter instead of an interesting feature. Thus, one can find hardly any presentation in the literature of voltage clamp K^+ currents for times long enough to quantitatively evaluate this effect. We hope, that the present theoretical study will be a stimulus for publication of such results, so that the course of the axolemmal K^+ conductance in the region near steady state can be evaluated in more detail than was possible above for *Loligo forbesi*.

After-effects of Trains of Action Potentials

As Frankenhaeuser and Hodgkin (1956) have shown, the net K^+ current during a succession of action potentials gives rise to measurable after-effects. These can be ascribed to shifts of the K^+ equilibrium potential due to accumulation of K^+ ions outside of the axolemma. Using the same number for the mean K^+ outflow per impulse of 4 pmole/cm^2 as these authors, a stimulation with 50/sec gives rise to a steady-state current $I_\infty = 19.3$ μamp/cm^2, whereas 125 impulses per sec constitute a current of $I_\infty = 48.2$ μamp/cm^2.

The steady-state K^+ accumulation in the GS space is established after about 30 to 50 msec and according to Eqs. (24) and (28) given by:

$$c(l)=I_\infty \cdot l/FAD. \tag{34}$$

If the stimulation experiment is done at $T=20$ °C (Frankenhaeuser & Hodgkin, 1956), then $D=1.7\times10^{-5}$ cm²/sec (Landolt-Börnstein, 1969). Taking again $A=0.01$ and $l=10$ μm, as found above for *Loligo forbesi*, we have with the above mean currents:

$$c_{50/\text{sec}}=1.2 \text{ mM}; \quad c_{125/\text{sec}}=2.9 \text{ mM}. \tag{35}$$

The corresponding shifts $[V_K-V_{Ko}]$ of the K^+ equilibrium potential can be computed from Eq. (30). Using $K_i=400$ mM and $V_{Ko}=-82$ mV at about $T=20$ °C (Hodgkin & Huxley, 1952*b*), we obtain with the above figures for c:

$$[V_K-V_{Ko}]_{50/\text{sec}}=1.8 \text{ mV}; \quad [V_K-V_{Ko}]_{125/\text{sec}}=4.4 \text{ mV}. \tag{36}$$

Shifts of the K^+ concentration near axolemma of a comparable magnitude as given in Eq. (35) were derived by Frankenhaeuser and Hodgkin (1956), applying a procedure of calibrating the after-effects with different external K^+ concentrations. These authors however did not allow for a resting K^+ concentration in the GS space different from the external medium, although they pointed out this possible source of error. Thus, a more detailed quantitative comparison with their experiments is not possible, unless there is a way to know the effect on $K_{e_o}(l)$ of different K^+ concentrations of the external medium. Certainly, the loss of K^+ ions by the Schwann cells, in addition to the leakage from the axon, should be an important factor in such an analysis.

Application of the Theory to Repolarization from the Steady State after Depolarization

In Appendix II the solution of Eqs. (14)–(18) and (20) is derived, if the initial condition is:

$$t=0; \quad c=d\cdot x.$$

The return of the K^+ concentration in the slits of the SCL to the resting values is described by:

$$\frac{c(x,t)}{d\cdot l}=\frac{x}{l}e^{-t/\tau}+\sum_{n=1}^{\infty}\frac{2\sin(\alpha_n x/l)}{N(\alpha_n)\sin\alpha_n}\,\frac{1-e^{-\left(\frac{1}{\tau}-K_n\right)t}}{1-\tau K_n}. \tag{37}$$

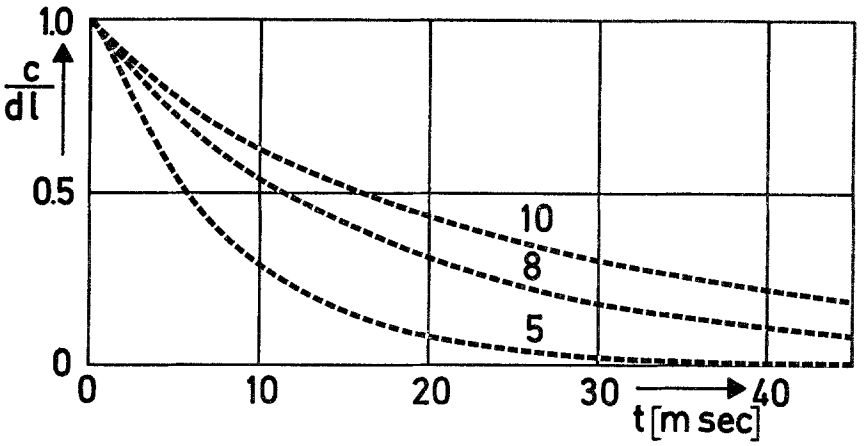

Fig. 5. Time course of decay of the K^+ excess concentration in the GS space after repolarization to the resting state according to Eq. (37). Curve parameter: l in μm. Other parameters are as in Fig. 4

Fig. 5 $c(l, t)$ for the following set of parameters: $T=20$ °C, i.e. $D=1.7\times10^{-5}$ cm²/sec; $\tau=1$ msec; $A=0.01$; $\delta=80$ Å. The curve parameters in Fig. 5 indicate l in μm.

Experiments corresponding to this set of parameters have been done by Frankenhaeuser and Hodgkin (1956). They observed at $T\approx20$ °C the return of the membrane potential and of other electrical characteristics of the axon to the resting state after shutting off a train of action potentials. It was shown that those parameters, which depend on the external K^+ concentration, and thus on the K^+ equilibrium potential, return to the resting state with a time constant of about 30 msec. For small deviation from the resting state, as is implied in these experiments, the K^+ equilibrium potential is a linear function of c [*see* Eq. (20)]. Fig. 5 shows that indeed the excess concentration of K^+ ions in the GS space, and with it the deviation of the K^+ equilibrium potential from the resting value, relaxes with a time constant of about 30 msec, if we choose $A=0.01$ and $l=10$ μm. These latter parameters are those which seem to describe best the effects of diffusion polarization in depolarizing voltage clamp experiments on giant axons of the same species of squid, as was discussed above.

Series Resistance

A system of channels of average length l and fractional area A, filled with seawater of specific resistance ρ, represents a resistance R_S in series to the membrane resistance given by:

$$R_S=\frac{l}{A}\rho. \tag{38}$$

With the geometrical characteristics $A=0.01$, $l=10$ μm found above for *Loligo forbesi*, we obtain $R_S=2.2\ \Omega\,cm^2$, where $\rho=22\ \Omega$ cm (Frankenhaeuser & Hodgkin, 1956) was used. This resistance R_S might contribute to the series resistance of a few $\Omega\,cm^2$, observed by different authors in voltage clamp experiments (*see* Cole, 1968). The contribution $R_S=2.2\ \Omega\,cm^2$, derived above, compares well with that determined by an independent electrophysiological procedure by Frankenhaeuser and Hodgkin (1956) who obtained $3.3\pm0.3\ \Omega\,cm^2$.

K^+-Transport in the Slits Including Electro-Kinetic Effects

Relations for Steady-State Convective Diffusion

As was discussed above, electro-osmotic volume flow accompanying current flow through the axolemma may have appreciable effects on K^+ transport through the SCL. For axons carrying large current densities and exhibiting only a small intra-slit volume, these effects should be taken into account. As was shown above, the main consequence of volume flow should be a widening of the thickness λ of the slits. A treatment of the time course of change of the geometry of the slits seems to be out of reach at present. Thus, in the following we shall consider steady-state convective diffusion of K^+ along the slits. The same geometrical model of the arrangement of slits as used above may be applied here. Only the width λ, which by Eq. (1) determines the surface fraction A of the slits, is now a function of the steady-state membrane current density I_∞.

The differential equation governing convective diffusion of K^+ ions through the slits reads (*cf.* Barry & Hope, 1969):

$$\frac{\partial c}{\partial t}=D\frac{\partial c^2}{\partial x^2}+\bar{q}\frac{\partial c}{\partial x}. \tag{39}$$

Here,

$$\bar{q}=q/A \tag{40}$$

is the volume flow per unit area of cross-section of the slits and is assumed positive, if directed outward. From Eq. (39), one obtains for steady state

$$\frac{\partial c}{\partial x}+\frac{\bar{q}}{D}c=d \tag{41}$$

where

$$d=I_\infty/FAD \tag{42}$$

is obtained from the second of the following boundary conditions

$$x=0\colon c=0 \tag{43}$$

$$x=l\colon I_\infty/AF=D\frac{\partial c}{\partial x}+\bar{q}c. \tag{44}$$

The solutions of Eqs. (41) through (44) reads:

$$c=\frac{I_\infty}{FAD}\frac{D}{\bar{q}}\left(1-e^{-\frac{\bar{q}}{D}x}\right). \tag{45}$$

Expansion of the exponent yields:

$$c=\frac{I_\infty}{FAD}x\left(1-\tfrac{1}{2}\frac{\bar{q}}{D}x+\tfrac{1}{6}\left(\frac{\bar{q}}{D}x\right)^2-\cdots\right). \tag{46}$$

Eq. (46) shows that for $\bar{q}x/D\ll 1$ the relation (34) of pure diffusion is obtained.

For an estimate on the higher terms in Eq. (46), we use again the data on electro-kinetic volume flow discussed above. For axons from *Loligo pealii*, we shall later use depolarizations as large as $V-V_r\approx 120$ mV. According to Eqs. (3), (5) and (6) this gives $q\approx 5\times 10^{-5}$ to 4×10^{-4} cm^3/cm^2 sec. For depolarizations of the above magnitude, we shall obtain $A\approx 0.1$, yielding $\bar{q}\sim 5\times 10^{-4}$ to 4×10^{-3} cm^3/cm^2 sec. Using $D=1.04\times 10^{-5}$ cm^2/sec, as applies to $T=4$ °C, the higher terms in Eq. (46) in this case amount to only $10^0/_0$. Thus, the contribution of convection turns out to be small and may be neglected for the present purposes. However, this estimate rests on electro-kinetic data obtained for another species of squid and should be reevaluated as soon as electro-kinetic data are available for axons from *Loligo pealii*. At present, the only effect of volume flow to consider is the change of width of the slits, whereas the transport through the enlarged slits may be treated as pure steady-state diffusion.

Application to Experiments on Axons from Loligo pealii

Since data on the electro-kinetic volume flow of axons from *Loligo pealii* are not available, the change of the geometrical dimensions of the slits due to volume flow can not be determined *a priori* for this species. Therefore, the geometrical parameters will be determined by adjustment for description of steady-state voltage clamp data. Thereafter, their order of magnitude may

be compared with that expected from application of electro-kinetic data from *Dosidicus gigas* axons. The procedure for evaluation of the geometrical parameter A/l from voltage clamp data is as follows.

The depolarization current $I_{K\,\mathrm{dep}}$ for steady state and the initial value $I_{K\,\mathrm{rep}}$ of the tail current after repolarization may be written as:

$$I_{K\,\mathrm{dep}} = g_K(V_{\mathrm{dep}} - V_K), \tag{47}$$

$$I_{K\,\mathrm{rep}} = g_K(V_{\mathrm{rep}} - V_K) \tag{48}$$

where V_{dep} and V_{rep} are the depolarization and repolarization potentials, respectively, of the voltage clamp, These equations may be solved for V_K. From V_K, the concentration $K_e(l)$ and, thus, $c(l)$ are obtained. According to Eq. (34) then, the parameter A/l may be computed from the steady-state depolarization current $I_{K\,\mathrm{dep}}$. Fortunately, data on the steady-state depolarization current and the initial tail current for two different axons over a fairly large range of membrane depolarizations are given by Adelman and Senft (1968) in their Figs. 3*b* and 5*b*. These experiments were done at $T=4$ °C; thus we have $D=1.04\times10^{-5}$ cm^2/sec (Landolt-Börnstein, 1969). As can be inferred from these data, the tail current is vanishingly small after repolarization to $V_{\mathrm{rep}}=-88$ mV from small depolarization (where K^+ accumulation is negligible). Thus, $V_{K\,o}$ is approximately given by V_{rep}.

Using $V_{K\,o}=-88$ mV and $K_i=400$ mM, Eq. (32) yields $K_{e\,o}(l)=10$ mM. According to these numbers, the difference between $K_{e\,o}(l)$ and the external K^+ concentration used by these authors turns out to be negligibly small for *Loligo pealii.*

In this respect axons from *Loligo pealii* seem to differ from those of *Loligo forbesi* (*see above*). This difference might be attributed to their differing thickness of the SCL, as reported by Geren and Schmitt (1954) and by Caldwell and Keynes (1960). In fact, our later evaluation of the geometrical parameter A/l for *L. pealii* will result in figures at least three times larger than those obtained above for *L. forbesi* by an equivalent procedure. This indicates a lesser efficiency of the SCL of axons from *L. forbesi* for removal of K^+ ions from the GS space. In addition, the presence of a larger area of Schwann cell membranes constituting the boundaries of the slits in *L. forbesi* axons might give rise to a larger efflux of K^+ ions from the Schwann cells into the intermembranous spaces of the SCL in the normal experimental situation of seawater as the external medium.

The data on magnitude and time constant of the rapid part of the K^+ outflow from ^{42}K-presoaked fibers (which is attributed to the SCL) from Shanes and Berman (1955) for *L. pealii* and from Caldwell and Keynes (1960) for *L. forbesi* are consistent with this interpretation.

Using $D=1.04\times10^{-5}$ cm^2/sec, $K_{e\,o}(l)=10$ mM, and $K_i=400$ mM, we have evaluated A/l for the experimental points of the two runs on axon 66–41 from Fig. 3*b* of Adelman and Senft (1968), and for the analogous data on axon

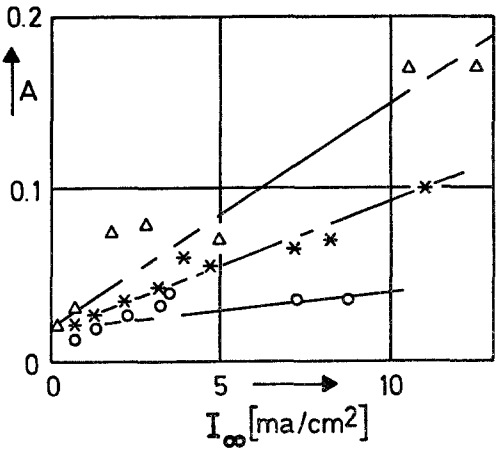

Fig. 6. Plot of parameter A versus steady-state K^+ current density I_∞ as described in the text. The points correspond to the original data from Adelman and Senft (1968): triangles, axon 66–41 "before"; open circles, same axon "after" (*see* Fig. 3*b*, l.c.); stars, axon 66–42 (*see* Fig. 5*b*, l.c.). Parameters used are: $T=4$ °C, $D=1.04\times10^{-5}$ cm²/sec; $l=5$ μ, $K_{e_o}=10$ mM, $K_i=400$ mM, i.e. $V_{K_o}=-88$ mV

66–42 from Fig. 5*b* (l.c). The results are given in Fig. 6, where for a more concrete picture of the physical situation we have specified $l=5$ μ.

As can be seen from this graph, the quantity A (or A/l) correlates linearly with the steady-state current density. This is to be expected, if the electro-kinetic volume flow is proportional to the charge flow through the axolemma. For very small currents, i.e. near the resting state, the data on Fig. 6 converge at $A\approx0.015$ to 0.02. At large currents, the width of the slits according to Fig. 6 may increase to up to 8 times the resting value. This is about the order of magnitude as estimated above by a comparison of the volume of the slits at the resting state with the electro-kinetic volume flow using some data from *Dosidicus gigas*. Thus, the proposed effect of a widening of the slits through the SCL by depolarizing currents appears very reasonable.

Upon hyperpolarization, the electro-kinetic volume flow is inward. This should lead to a collapse of the lumen of the slits. There is the following evidence that this might be the case. Adelman and Palti (1969) have interpreted effects of prolonged hyperpolarizations of axons from *Loligo pealii* as due to a draining of K^+ ions from the Frankenhaeuser-Hodgkin space. The time constant of this process is 150 to 300 msec according to their figures. On the other hand, the time constant for K^+ redistribution after depolarizing currents was given as 5 to 10 msec by the same authors (Adelman & Palti, 1972). This difference of K^+ redistribution times is reflected by parameters P_{K_s} about an order of magnitude different (at nearly equal θ)

used by those authors to describe these two sets of experiments in terms of the Frankenhaeuser-Hodgkin model. This difficulty may be resolved by the use of Eqs. (12) and (25), invoking the proposed effect of volume flow on A, as follows. Using $D=1.04\times10^{-5}$ cm^2/sec, $l=5$ μ and $A=0.015$, we obtain from Eqs. (12) and (25): $\tau_{Ch}\approx12$ msec. This is an upper limit, as the contribution of convection would decrease the time of K^+ redistribution. Incidentally, this number justifies the assumption of steady state in the application of the theory to the data presented in Fig. 6. If now the parameters $l=5$ μ and $\delta=8\times10^{-7}$ cm are kept fixed, but the width of the slits is changed for instance from $A=0.015$ to $A=0.001$, then τ_{Ch} would, according to Eqs. (12) and (25), increase by a factor of four. This effect might contribute to an explanation of the discrepancy on the time constants applicable for hyper- and depolarization. For a more quantitative description, the time course of geometrical changes of the intermembranous spaces in the SCL has to be evaluated.

The above predictions of the theory might be checked by an independent determination of the contribution of the SCL to the series resistance of the axon. Using a specific resistance of seawater of $\rho=22$ Ω cm (Frankenhaeuser & Hodgkin, 1956; Cole, 1968) and $A/l\approx30$ cm^{-1}, as evaluated in Fig. 6 for the resting state, Eq. (38) yields $R_S\approx0.8$ Ω cm^2. At the steady state of a strongly depolarizing voltage clamp, this series resistance should have decreased to about $R_S\approx0.1$ Ω cm^2. Upon prolonged hyperpolarization R_S should rise considerably beyond these figures. Detailed experimental data on the series resistance at different experimental conditions, thus, would be of considerable interest.

A further experimental check might come forward from electron-microscopic investigations of the SCL. A first indication in favor of the concept presented above is the observation of Geren and Schmitt (1954) of a widening of the lumen of the slits in Ca^+-deficient media. Further data clearly are very desirable.

It is of interest to deduce from Fig. 6 the steady state K^+ conductance of the axolemma. Within the accuracy of the present theory, this quantity does not contain the effects of K^+ accumulation in the GS space anymore. Thus, it may profitably be compared with the K^+ conductance of the axon in KCl-seawater, i.e. in seawater where all the Na^+ ions are replaced by K^+ ions and, therefore, K^+ accumulation in the GS space has practically no effect on V_K.

Moore *et al.* (1966) have given measurements of K^+ currents over a fairly broad range of membrane potentials for an axon of *Loligo pealii*, both in seawater and KCl-seawater. Unfortunately, the tail currents after re-

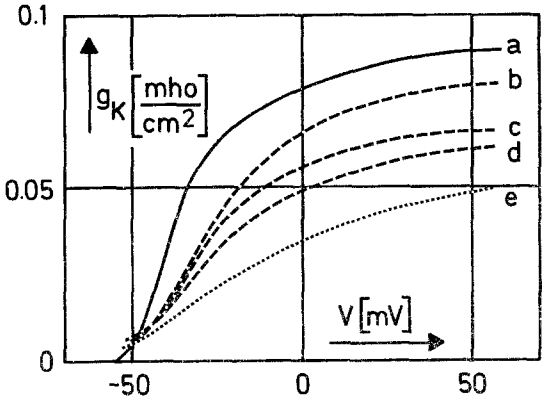

Fig. 7. Steady-state K^+ conductances from data of Moore *et al.* (1966) for seawater (curves "b" through "e") and KCl-seawater (curve "a") derived as described in the text. Parameters: $T=10$ °C, $D=1.3\times10^{-5}$ cm²/sec, $l=5$ μ, $K=10$ mM, $K_i=400$ mM. A as a function of steady-state current I is taken from Fig. 6. Curve labels: "a" KCl-seawater, "e" = Hodgkin-Huxley conductance (fixed $V_{K_o}=-88$ mV), "b" corresponds to axon 66–41 "after", "c" to axon 66–42, "d" to axon 66–41 "before" (*see* Fig. 6)

polarization have not been reported in this case. With such complete data lacking at present, we shall derive the K^+ conductances from the data of Moore *et al.* (1966) using the dependences of A/l on steady-state current density as derived for different axons of the same species of squid from the measurements of Adelman and Senft (1968) and shown in our Fig. 6. This tentative comparison is shown in Fig. 7. Here the curve labeled with "e" is the K^+ conductance in seawater evaluated from Fig. 2 of Moore *et al.* (1966), according to the Hodgkin-Huxley procedure without regard for a possible K^+ accumulation, i.e. using a time independent $V_K=-88$ mV in Eq. (31). Curves "b", "c" and "d" represent the K^+ conductances for the same axon in seawater as given by Eqs. (30), (31) and (34), where A/l in dependence on $I_{K\infty}$ was taken from the curves in Fig. 6. Here $D=1.3\times10^{-5}$ cm²/sec (corresponding to $T=10$ °C of the experiments of Moore *et al.*, 1966), $K_{e_o}=10$ mM, and $K_i=400$ mM were used. As can be seen from Fig. 7, any of the geometrical characteristics taken from the two axons measured by Adelman and Senft (1968), lead to marked deviations of the axolemmal K^+ conductance from the Hodgkin-Huxley conductance. Whereas the latter takes about 110 mV for the transition from 10% to 90% of the maximal conductance, the conductances represented by curves b, c and d in Fig. 7 rise within 50 to 60 mV from 10 to 90%. The absolute values of the K^+ conductance too, are considerably higher than the "Hodgkin-Huxley" conductance (curve "e"). Thus, any molecular theory of the voltage dependence of the steady-state axolemmal

K^+ conductance, which fits the Hodgkin-Huxley conductance, is off the goal by quite a margin.

It has been noted by several authors (*see*, for instance, Fig. 8 in Lecar *et al.*, 1967) that the steady-state K^+ conductance for an axon in KCl-seawater deviates grossly from the Hodgkin-Huxley K^+conductance. The same is evident from a comparison of curves "a" and "e" in Fig. 7. Here, curve "a" represents the K^+ conductance for KCl-seawater derived from Fig. 2 of Moore *et al.*, (1966) according to Eqs. (30), (31) and (34). In this derivation we have used $D=1.3\times10^{-5}$ cm^2/sec, $l=5$ μm, $A=0.03$, $K_e=460$ mM, and $K_i=400$ mM, the latter figures giving $V_{Ko}=3.4$ mV. The circumstance that the zero-current potential in the measurements of Moore *et al.* (1966) was not equal to $V_{Ko}=3.4$ mV, has been attributed by the above authors to the special conditions of the sucrose gap voltage clamp. It has been allowed for in curve "a", by shifting the experimental current-voltage curve for KCl-seawater of Moore *et al.* (1966) such that the zero-current potential is equal to 3.4 mV. The choice of the above parameters is not at all critical. For instance, evaluation of the K^+ conductance in KCl-seawater with fixed $V_K=3.4$ mV gives practically the same curve as curve "a". This is to be expected, since at high K_e the equilibrium potential is very insensitive to any changes of the K^+ concentration in the GS space due to current flow.

A comparison of the curves in Fig. 7 shows that consideration of K^+ accumulation in the SCL during current flow for an axon in seawater leads to steady-state K^+ conductances approaching that for an axon in KCl-seawater. Thus, the possibility arises that the axolemmal steady-state K^+ conductance has the same dependence on membrane potential for an axon in seawater and for an axon in KCl-seawater. Such a situation would simplify considerably any concept on the molecular K^+ conductance mechanism of the axolemma. Unfortunately, the accuracy of the data presently available does not warrant a firm conclusion on this question yet. It is hoped that experimental data on voltage clamp currents for seawater and KCl-seawater, including the tail currents on the same axon will be stimulated by the present theory so that this basic question may be answered.

Conclusion

In the present paper the effect of K^+ accumulation in the GS space on the K^+ current has been treated. It could be shown for voltage clamp experiments in seawater using small depolarizations that the main consequences of this accumulation are an increase of the magnitude, and a slower temporal rise of the K^+ conductance of the axolemma as compared to the Hodgkin-

Huxley K^+ conductance. These are quite marked effects, as shown for axons of *Loligo forbesi.*

Adjusting in essence only two geometrical parameters, i.e. the length l of the slits and the fractional surface area A occupied by the slits, a number of effects could be described: the change of the tail currents after repolarization at different times after a depolarizing voltage clamp, the time constant of decay of the after-effects due to a succession of action potentials, and the magnitude of the series resistance of the SCL.

Furthermore, strong evidence has been assembled that, depending on the type of axon and the magnitude of the depolarization, the effects of electro-kinetic volume flow are appreciable. These effects have been taken into account by allowing for a change of the geometrical parameters of the intermembranous spaces of the SCL during current flow.

Applied to voltage clamp data on axons from *Loligo pealii*, this concept allowed a quantitative description of the dependence of the tail currents on the magnitude of previous depolarization.

After considering in this way the effect of K^+ accumulation on the voltage dependence of the steady-state K^+ current in seawater, the K^+ conductance of the axolemma proper may be evaluated. It turns out to be very similar in its dependence on membrane potential to the K^+ conductance for the axon in KCl seawater. This seems to resolve an early noted discrepancy and is a result of considerable interest from point of view of a mechanistic interpretation.

Some predictions amenable to experimental test can be made on the basis of this theory. The series resistance due to the SCL should be smaller in *Loligo pealii* than in *Loligo forbesi.* It should depend strongly on de- or hyperpolarization of the axon.

The use of different geometrical parameters for *Loligo forbesi* and *Loligo pealii* should show up also in other features discussed in the text. This difference seems fully consistent with the observed difference of thickness of the SCL. The theoretical analysis is hampered by a lack of pertinent experimental data, and is hoped to be a stimulus for such work. Most important would be an investigation on the electro-kinetic volume flow in *Loligo* axons. Very desirable also are data for one and the same axon on: (a) voltage clamp currents in seawater including the tail currents; (b) voltage clamp currents in KCl seawater; (c) determination of the series resistances under different experimental conditions; (d) quantitative electron-microscopic investigation on the structure of the SCL. If these data were available, then the quantitative evaluation of the K^+ conductance of the axolemma proper would be

possible as a goal for theories on the molecular mechanism of the K^+ conductance.

The author wishes to thank Drs. K. S. Cole, C. W. Armstrong, W. J. Adelman, Jr. and L. J. Mullins for stimulating and critical discussion, in particular on occasion of a meeting on "Ion Flow in Nerve Membranes" April 1971 in Birmingham, Alabama.

Appendix I

Solution of the Diffusion Equation for Depolarization

Using the Laplace-transform $\bar{c}(x, s)$ from $c(x, t)$, we have instead of Eqs. (14) and (16) through (19):

$$\frac{d_2\bar{c}}{dx^2}-\frac{s}{D}\bar{c}=0 \tag{A.1}$$

$$x=0\colon \bar{c}=0 \tag{A.2}$$

$$x=l\colon \frac{d\bar{c}}{dx}-d\sum_{m=0}^{4}(-\rho)^m\binom{4}{m}\frac{1}{s+\frac{m}{\tau}}+as\bar{c}=0 \tag{A.3}$$

where

$$d=\frac{I_\infty}{FAD} \tag{A.4}$$

$$a=\frac{\delta}{AD}. \tag{A.5}$$

The general solution of Eq. (A.1) is

$$\bar{c}=C_1\cosh\left(\sqrt{\frac{s}{D}}x\right)+C_2\sinh\left(\sqrt{\frac{s}{D}}x\right). \tag{A.6}$$

From Eqs. (A.2) and (A.6), we obtain $C_1=0$. From Eqs. (A.3) and (A.6), the constant C_2 is obtained, yielding

$$\bar{c}=\sum_{m=0}^{4}(-\rho)^m\binom{4}{m}\bar{c}_m \tag{A.7}$$

where

$$\bar{c}_m=\frac{d}{s+\frac{m}{\tau}}\cdot\frac{\sinh\left(\sqrt{\frac{s}{D}}x\right)}{\sqrt{\frac{s}{D}}\cosh\left(\sqrt{\frac{s}{D}}l\right)+as\sinh\left(\sqrt{\frac{s}{D}}l\right)}. \tag{A.8}$$

The inverse of the Laplace-transform of Eq. (A.7) can be written as

$$c(x,t)=\sum_{m=0}^{4}(-\rho)^m\binom{4}{m}c_m(x,t) \tag{A.9}$$

where

$$c_m(x,t)=\frac{1}{2\pi i}\int_{\gamma-i\infty}^{\gamma+i\infty}ds\cdot e^{st}\cdot\bar{c}_m(x,s). \tag{A.10}$$

The first term in the sum of Eq. (A.9) corresponds to immediate onset of a constant current: $I_K(t)=I_\infty$, i.e. $\tau=0$ in Eq. (A.10) with (A.8). We first derive this solution $c_0(x,t)$ as follows. After substituting Eq. (A.8) with $m=0$ into Eq. (A.10), the poles of the integrand are

$$s=0 \text{ with residue } d\cdot x \tag{A.11}$$

and

$$s_n=-\frac{D\alpha_n^2}{l_2} \tag{A.12}$$

where α_n are the solutions of the trancendental equation

$$\alpha\, tg\alpha=\frac{l}{aD}=\frac{Al}{\delta}. \tag{A.13}$$

To find the residues at the poles given by Eq. (A.12), we form the following expression and substitute $s=D\mu^2$

$$\begin{aligned}&\left[s\frac{d}{ds}\left\{\sqrt{\frac{s}{D}}\cosh\left(\sqrt{\frac{s}{D}}l\right)+as\cdot\sinh\left(\sqrt{\frac{s}{D}}l\right)\right\}\right]_{s=-D\alpha_n^2/l^2}\\&=\left[\frac{\mu}{2}\frac{d}{d\mu}\{\mu\cosh(\mu l)+aD\mu^2\sinh(\mu l)\}\right]_{\mu=i\alpha_n/l}\\&=\frac{1}{2l}i\alpha_n\left[\left(1-\frac{aD\alpha_n^2}{l}\right)\cos\alpha_n-\left(1+\frac{2aD}{l}\right)\alpha_n\sin\alpha_n\right].\end{aligned} \tag{A.14}$$

Using the results given by Eq. (A.11) and (A.14) with (A.13), one may write the complex integral of Eq. (A.10) with Eq. (A.8) for the case $m=0$ as

$$c_0(x,t)=dx-\sum_{n=1}^{\infty}2\cdot l\cdot d\frac{\sin(\alpha_n x/l)}{N(\alpha_n)\sin\alpha_n}e^{-K_nt} \tag{A.15}$$

where

$$N(\alpha_n)=\frac{\delta\alpha_n^2}{Al}\left(1+\frac{\delta\alpha_n^2}{Al}\right)+\alpha_n^2 \tag{A.16}$$

$$K_n=D\alpha_n^2/l^2. \tag{A.17}$$

The higher terms in Eq. (A.9) can be constructed from c_o by an application of the convolution theorem of the Laplace-transformation. This theorem states that the inverse of a product of two Laplace-transforms $\bar{f}_1(s)$ and $\bar{f}_2(s)$ is the convolution of the two original functions $f_1(t)$ and $f_2(t)$ (Doetsch, 1950):

$$\frac{1}{2\pi i}\int_{\gamma-i\infty}^{\gamma+i\infty} ds \cdot e^{ts}\bar{f}_1(s)\bar{f}_2(s)=\int_0^t du f_1(u)\cdot f_2(t-u). \tag{A.18}$$

The higher terms of Eq. (A.8) may be written as

$$\bar{c}_m(x,s)=\frac{s}{s+\frac{m}{\tau}}\bar{c}_0(x,s)=\bar{c}_0-\frac{m/\tau}{s+\frac{m}{\tau}}\bar{c}_0. \tag{A.19}$$

Thus, if we use $\bar{f}_1(s)=\bar{c}_o$ and $\bar{f}_2(s)=\frac{m}{\tau}\frac{1}{s+m/\tau}$ in Eq. (A.18) we obtain from Eq. (A.19)

$$c_m(x,t)=c_0(x,t)-\frac{m}{\tau}\int_0^t du\cdot c_0(x,u)\,e^{-\frac{(t-u)}{\tau/m}}. \tag{A.20}$$

Introducing Eqs. (A.15) through (A.17) into Eq. (A.20), and performing the integration yields

$$c_m(x,t)=c_0-d\cdot x\left(1-e^{-\frac{mt}{\tau}}\right)+2\cdot l\cdot d\sum_{n=1}^{\infty}\frac{\sin(\alpha_n x/l)}{N(\alpha_n)\sin\alpha_n}e^{-K_n t}\frac{1-e^{-\left(\frac{m}{\tau}-K_n\right)t}}{1-\frac{\tau}{m}K_n}. \tag{A.21}$$

The summation of Eq. (A.9) finally yields

$$c(x,t)=(c_0-dx)(1-\rho)^4+d\cdot x\left(1-\rho e^{-\frac{t}{\tau}}\right)^4+\sum_{n=1}^{\infty}2l\cdot d\frac{\sin(\alpha_n x/l)}{N(\alpha_n)\sin\alpha_n}e^{-K_n t}\sum_{m=0}^{4}T_{mn} \tag{A.22}$$

where

$$T_{mn}=(-\rho)_m\binom{4}{m}\frac{1-e^{-\left(\frac{m}{\tau}-K_n\right)t}}{1-\frac{\tau}{m}K_n}. \tag{A.23}$$

It is verified easily that Eqs. (A.22) and (A.23) fulfill the partial differential Eq. (14) and the initial and boundary conditions (16) through (19). The initial condition for the partial solution $c_o(x, t)$ was verified by numerical inspection (*see* Fig. 2).

Appendix II

Solution of the Diffusion Problem for Repolarization

In this case, the initial condition is

$$t=0:\ c=d\cdot x. \tag{A.24}$$

The boundary conditions read

$$x=0\colon c=0 \tag{A.25}$$

$$x=l\colon \frac{\partial c}{\partial x}-d e^{-t/\tau}+a\frac{\partial c}{\partial t}=0. \tag{A.26}$$

The Laplace-transforms of these equations and Eq. (14) are

$$\frac{d^2\bar{c}}{dx^2}-\frac{s}{D}\bar{c}+\frac{d\cdot x}{D}=0 \tag{A.27}$$

$$x=0\colon \bar{c}=0 \tag{A.28}$$

$$x=l\colon \frac{d\bar{c}}{dx}-\frac{d}{s+\frac{1}{\tau}}+as\bar{c}-ad\cdot l=0. \tag{A.29}$$

It is verified easily, that Eqs. (A.27) through (A.29) are fulfilled by

$$\bar{c}(x,s)=\left(-\frac{d}{s}+\frac{d}{s+\frac{1}{\tau}}\right)\frac{\sinh\left(\sqrt{\frac{s}{D}}x\right)}{\sqrt{\frac{s}{D}}\cosh\left(\sqrt{\frac{s}{D}}l\right)+as\sinh\left(\sqrt{\frac{s}{D}}l\right)}+\frac{xd}{s}. \tag{A.30}$$

With the notations of Appendix I, this can be written

$$\bar{c}(x,s)=-\bar{c}_0(x,s)+\bar{c}_1(x,s)+\frac{xd}{s}. \tag{A.31}$$

The inverse of this Laplace-transform is

$$c(x,t)=-c_0(x,t)+c_1(x,t)+x\cdot d. \tag{A.32}$$

With the use of Eqs. (A.15) and (A.21), this equation yields finally

$$\frac{c(x,t)}{l\cdot d}=\frac{x}{l}e^{-t/\tau}+\sum_{n=1}^{\infty}2\frac{\sin(\alpha_n x/l)}{N(\alpha_n)\sin\alpha_n}e^{-K_n t}\frac{1-e^{-\left(\frac{1}{\tau}-K_n\right)t}}{1-\tau K_n}. \tag{A.33}$$

References

Adam, G. 1970. Theory of nerve excitation as a cooperative cation exchange in a two-dimensional lattice. *In:* Physical Principles of Biological Membranes. F. Snell, J. Wolken, G. Iversen and J. Lam, editors. p. 35. Gordon and Breach Science Publishers, New York

Adam, G. 1971. A molecular mechanism for regulation of the K^+ current through the axon membrane. *In:* First European Biophysics Congress. E. Broda, A. Locker and H. Springer-Lederer, editors. Proceedings, Vol. V, p. 193. Verlag der Wiener Medizinischen Akademie, Vienna

Adelman, W. J., Palti, V. 1969. The effects of external potassium and long duration voltage conditioning on the amplitude of sodium currents in the giant axon of the squid, *Loligo pealii. J. Gen. Physiol.* **54**:589

Adelman, W. J., Palti, Y. 1972. The role of periaxonal and perineuronal spaces in modifying ionic flow across neural membranes. *In:* Current Topics in Membranes and Transport. F. Bronner and A. Kleinzeller, editors. p. 199. Academic Press Inc., New York

Adelman, W. J., Senft, J. P. 1968. Dynamic asymmetries in the squid axon membrane. *J. Gen. Physiol.* **51**:102*s*

Barry, P. H., Hope, A. B. 1969. Electroosmosis in membranes: Effects of unstirred layers and transport numbers. *Biophys. J.* **9**:700, 729

Blumenthal, R., Changeux, J.-P., Lefevre, R. 1970. Membrane excitability and dissipative instabilities. *J. Membrane Biol.* **2**:351

Caldwell, P. C., Keynes, R. D. 1960. The permeability of the squid giant axon to radioactive potassium and chloride ions. *J. Physiol.* **154**:177

Carslaw, H. S., Jaeger, J. C. 1959. Conduction of Heat in Solids. Second edition, p. 173. Clarendon Press, Oxford

Cohen, L. B. 1970. Light scattering changes during axon activity. *In:* Permeability and Function of Biological Membranes. L. Bolis, A. Katchalski, R. D. Keynes, W. R. Loewenstein and B. A. Pethica, editors. p. 318. North-Holland Publishing Co., Amsterdam

Cole, K. S. 1968. Membranes, Ions and Impulses. p. 350. California University Press, Berkeley.

Cole, K. S., Moore, J. W. 1960. Potassium ion current in the squid giant axon: Dynamic characteristic. *Biophys. J.* **1**:1

Doetsch, G. 1950. Handbuch der Laplacetransformation. Vol. I, p. 256, Verlag Birkhäuser, Basel

Frankenhaeuser, B., Hodgkin, A. L. 1956. The after-effects of impulses in the giant nerve fibres of *Loligo. J. Physiol.* **131**:341

Geren, B. B., Schmitt, F. O. 1954. The structure of the Schwann-cell and its relation to the axon in certain invertebrate nerve fibers. *Proc. Nat. Acad. Sci.* **40**:863

Gerthsen, C. 1963. Physik. 7th. Ed., p. 70. Springer-Verlag, Berlin

Hill, T. L., Chen, Y. 1970. Cooperative effects in models of steady-state transport across membranes. III. Simulation of potassium ion transport in nerve. *Proc. Nat. Acad. Sci.* **66**:607

Hill, T. L., Chen, Y. 1971. On the theory of ion transport across the nerve membrane, potassium ion kinetics and cooperativity. *Proc. Nat. Acad. Sci.* **68**:1711, 2488

Hodgkin, A. L., Huxley, A. F. 1952*a*. Currents carried by sodium and potassium ions through the membrane of the giant axon of *Loligo. J. Physiol.* **116**:449

Hodgkin, A. L., Huxley, A. F. 1952*b*. The components of membrane conductance in the giant axon of *Loligo. J. Physiol.* **116**:473

Hodgkin, A. L., Huxley, A. F. 1952*c*. The dual effect of membrane potential on sodium conductance in the giant axon of *Loligo. J. Physiol.* **116**:497

Hodgkin, A. L., Huxley, A. F. 1952*d*. A quantitative description of membrane current and its application to conduction and excitation in nerve. *J. Physiol.* **117**:500

Landolt-Börnstein. 1969. Zahlenwerte und Funktionen. 6th Ed., Vol. II, Pt. 5a, p. 620f. K. Schäfer, Herausg., Berlin

Lecar, H., Ehrenstein, G., Binstock, L., Taylor, R. E. 1967. Removal of potassium negative resistance in perfused squid giant axons. *J. Gen. Physiol.* **50**:1499

Moore, J. W., Anderson, N., Blaustein, M., Takata, M., Lettvin, J. Y., Pickard, W. F., Bernstein, T., Pooler, J. 1966. Alkali cation selectivity of squid axon membrane. *Ann. N. Y. Acad. Sci.* **137**:818

Rojas, E., Ehrenstein, G. 1965. Voltage clamp experiments on axons with potassium as the only internal and external cation. *J. Cell. Comp. Physiol.* **66**:71

Schlögl, R. 1964. Stofftransport durch Membranen. p. 44, Dr. D. Steinkopff Verlag, Darmstadt

Shanes, A. M., Berman, M. D. 1955. Kinetics of ion movement in the squid giant axon. *J. Gen. Physiol.* **39**:279

Vargas, F. F. 1968. Water flux and electrokinetic phenomena in the squid axon. *J. Gen. Physiol.* **51**:123s

Vetter, K. J. 1961. Elektrochemische Kinetik. p. 153. Springer-Verlag, Berlin

Villegas, G. M., Villegas, R. 1964. Extracellular pathways in the peripheral nerve fibre: Schwann-cell layer permeability to thorium dioxide. *Biochim. Biophys. Acta* **88**:231

Villegas, G. M., Villegas, R. 1968. Ultrastructural studies of the squid nerve fibers. *J. Gen. Physiol.* **51**:44s

Villegas, G. M., Villegas, R. 1960*a*. The ultrastructure of the giant nerve fiber of the squid: Axon-Schwann cell relationship. *J. Ultrastruct. Res.* **3**:362

Villegas, J. 1972. Axon-Schwann-cell interaction in the squid nerve fibre. *J. Physiol.* **225**:275

Villegas, R., Barnola, F. V. 1961. Characterization of the resting axolemma in the giant axon of the squid. *J. Gen. Physiol.* **44**:963

Villegas, R., Caputo, C., Villegas, L. 1962. Diffusion barriers in the squid nerve fiber. *J. Gen. Physiol.* **46**:245

Villegas, R., Villegas, G. M. 1960*b*. Characterization of the membranes in the giant nerve fiber of the squid. *J. Gen. Physiol.* **43**:73*s*